Responses to comments by reviewer #1

Marco Antonellini (Referee)

m.antonellini@unibo.it

Ref: SE-2020-76-RC1

The preprint paper "Measuring hydraulic fracture apertures: a comparison of methods" by Chaojie Cheng, Sina Hale, Harald Milsch, Philipp Blum deals with a comparison of three methods used to estimate the mechanical and hydraulic aperture of fractures under controlled lab conditions. The paper is well written, and the figures are nicely drafted and easy to understand. I think that this is going to be an important addition to the experimental literature aimed at quantifying fracture permeability with laboratory methods. I have some comments about the way the methods are presented and the context in which the results obtained are relevant. Some elaboration of the authors on the following issues might help strengthen the paper:

We sincerely thank Marco Antonellini for his constructive comments and valuable suggestions, which greatly helped to improve the manuscript's quality. In the following, we provide a point-by-point response to the comments, where comments are in black, and our responses are in red. In addition, any changes regarding ''author responses to reviewer #1'' applied in the revised manuscript are also colored in red.

(1) The aperture measured at the surface of an outcrop might not have anything to do with the aperture measured at reservoir or aquifer conditions, because of the stress state at depth. This issue has always hampered the recognition of any validity of fracture aperture measurements from cores, lab experiments, or outcrops.

Response: We certainly agree with this fact which is (once more) also evident from Fig. 4. To recall, the main goal of this study was to compare hydraulic apertures determined with two portable methods to direct measurements using a flow-through apparatus. The comparison was performed for the same set of samples and at identical environmental conditions (ambient temperature and pressure). It is well understood that characterizing the hydraulic aperture of fractures at depth from measurements taken at the surface of an outcrop demands information on the mechanical response of a fracture to stress. This extrapolation will require the continued application of rock mechanical/physical devices like the one used in this study and measurements of the type displayed in Fig. 4. We have addressed this important point in *Lines 43-47* and also added corresponding statements in the conclusions section (*Lines 404-408*) that also relate to the second point in comment (2) below.

(2) The boundary conditions during a measurement made with the Tiny Perm might lead to a non-uniform sampling of the fracture and to erroneous results. For example, there might be gas slippage from the fracture at the end of the nozzle. In this case the permeability measurement is affected by an asymmetry of the flow field, so that the real hydraulic aperture of the fracture is not obtained. The fact that the different methods give similar results does not mean that they can be extended beyond the experimental conditions tested.

Response: We agree with both points. Regarding the first point we have clarified this issue in *Lines 215-218*. Regarding the second point we have added a corresponding statement to the manuscript in *Lines 404-405*.

(3) In the case of measurements made on fractures with smooth surfaces shut by the confining pressure, the instrument might read matrix permeability and not the hydraulic aperture of the fracture.

Response: The matrix permeability of the samples used in this study is in the order of 10^{-18} m^2 as derived from previous flow-through measurements (e.g., Blöcher et al., 2009; *citation added in Section 2.1 and the list of references*). In contrast and at ambient pressure conditions, the respective permeability of all samples was measured to be at least two orders of magnitude larger than the corresponding matrix permeability. We agree, that fractures may close at elevated confining pressure and we have clearly stated the requirements for the applicability of the data evaluation procedure in the *updated Section 2.2.1*.

(4) I find the statement in the conclusion "For such purposes, this study shows that the transient air flow permeameter offers a fast and highly efficient approach for accurate hydraulic aperture determination" very strong and a bit misleading. The number of samples tested and the experimental conditions (stress state, scale, and dimensions) are rather limited for such a strong statement. The air flow permeameter is as good as the calibration curve that allows to empirically correlate the pressure decay to the hydraulic aperture. Given the peculiar and heterogeneous flow field of the permeameter within the fracture, these empirical correlations are likely to vary a lot from sample to sample.

Response: This comment relates to Eq. (5) and the corresponding comment below. We agree that the number of samples tested and their length scale is rather limited. However, several types of single fractures (aligned, displaced, rough, smooth) were tested and the match between hydraulic apertures determined by the FTA and the TP was found to be very good (at corresponding pressure conditions). This result was obtained with a single calibration that relies on the parallel-plate assumption. Nonetheless, we have rephrased the corresponding statement accordingly in the conclusions section (*Lines 395-396*).

Some technical remarks:

Line 18 "…aperture differences between samples are merely reproduced qualitatively." I don't find this sentence clearly written.

Response: We have rephrased this sentence in *Lines 18-19*.

Line 26 Also CO2 injection site characterization might benefit from your work…

Response: Agreed and added to the revised manuscript in *Line 26*.

Lines 113-116 Some references would help making clear what you have done here.

Response: We have revised this paragraph for clarification and added three references in *Line 129*.

Line 126 I would change the sentence like this: "…pressure profile through time measured by the instrument pressure transducer and flowmeters"

Response: We have rephrased the statement accordingly in *Lines 142-143*

Eq. (5) $T = -1.5\log_{10}(a_{TP})+8.29$ Given the peculiar and heterogeneous flow field of the permeameter within the fracture, this empirical correlation is likely to vary a lot from sample to sample.

Response: This empirical correlation was originally derived based on measuring known fracture apertures between parallel-plate fractures. In this simplified case, mechanical apertures are equal to hydraulic apertures. In fact, the device works with this single empirical correlation to determine

the hydraulic aperture of "natural" fractures. Thus, one main goal of the present work was to demonstrate whether this simple approach properly works on rough fractures deviating from the idealized case. To our knowledge, no validation and also no precision assessment have been performed on rough fractures yet. We have added one related statement in **Lines 158-159**.

Line 165 Is this (a_h) consistent with the terminology used before?

Response: a_{TP}, a_{FTA}, and a_h all represent hydraulic fracture aperture. We used different notations to differentiate the results derived from different methods. a_{TP} represents hydraulic aperture measured with the Tiny Perm 3, a_{FTA} is the one obtained with the flow-through apparatus and a_h is derived based on the empirical correlations between hydraulic and mechanical apertures in Table 1. The notation (a_h) is therefore consistent with the terminology used throughout the paper.

Lines 224-225 These fractures are likely closed and the TP measures matrix permeability

Response: As mentioned before (comment 3), all fractures are open to a certain degree since the measured sample permeability is always significantly larger than the matrix permeability of these samples.

Fig. 7 What are the black dots in the graph above measurements FF2, FF3, FF4, and FOF4?

Response: We have updated the corresponding **figure caption** for clarification.

Line 262 Width or length?

Response: Here, the width of the fracture represents the fracture profile on the sample ends, which is equal to the sample diameter. In contrast, the fracture length is equal to the sample length. The term 'width' was therefore retained.

Fig. 9 What are the black dots above the boxplots?

Response: Same as Fig. 7. Again, we have updated the corresponding **figure caption** for clarification.

Lines 273-275 This sentence is not clear, please explain.

Response: We have revised the corresponding statements for clarification in **Lines 321-324**.

Lines 338-339 "…the derived mean and…" This is not clear what it means.

Response: Conclusion (3) has been revised for clarification in **Lines 389-391**.

Line 341 You talk about temperature in the conclusions but I am not sure you have investigated this in your experiments.

Response: Agreed. The statement has been deleted.

References added in the revised manuscript:

Blöcher, G., Zimmermann, G., & Milsch, H. (2009). Impact of poroelastic response of sandstones on geothermal power production. Pure and Applied Geophysics, 166(5-7), 1107-1123. https://doi.org/10.1007/s00024-009-0475-4

Brown, S., & Smith, M. (2013). A transient-flow syringe air permeameter. Geophysics, 78(5), D307-D313. https://doi.org/10.1190/Geo2012-0534.1 (was already cited in the ms)

Bruines, P. (2003). Laminar ground water flow through stochastic channel networks in rock, (Doctoral dissertation). Lausanne: EPFL.

Filomena, C., Hornung, J., & Stollhofen, H. (2014). Assessing accuracy of gas-driven permeability measurements: a comparative study of diverse Hassler-cell and probe permeameter devices. Solid Earth, 5(1), 1-11. https://doi.org/10.5194/se-5-1-2014

Ukar, E., Laubach, S. E., & Hooker, J. N. (2019). Outcrops as guides to subsurface natural fractures: Example from the Nikanassin Formation tight-gas sandstone, Grande Cache, Alberta foothills, Canada. Marine and Petroleum Geology, 103, 255-275.

Watkins, H., Bond, C. E., Healy, D., & Butler, R. W. (2015). Appraisal of fracture sampling methods and a new workflow to characterise heterogeneous fracture networks at outcrop. Journal of Structural Geology, 72, 67-82. https://doi.org/10.1016/j.jsg.2015.02.001 (was already cited in the ms)

Zeeb, C., Gomez-Rivas, E., Bons, P. D., & Blum, P. (2013). Evaluation of sampling methods for fracture network characterization using outcrops. AAPG bulletin, 97(9), 1545-1566. https://doi.org/10.1306/02131312042 (was already cited in the ms)

Responses to comments by reviewer #2

Miller Zambrano (Referee)

miller.zambrano@unicam.it

Ref: SE-2020-76-RC2

Measuring hydraulic fracture apertures: a comparison of methods: This is my first time reviewing this manuscript. The topic is of remarkable interest, and it has been widely investigated from different points of views implementing several techniques and approaches. Therefore, the expectations from this manuscript are quite high. In general, the manuscript describes a series of methods for estimating the hydraulic aperture and makes a comparison among them. I have just some considerations that can improve the quality of the manuscript:

We sincerely thank Miller Zambrano for his constructive comments and valuable suggestions of additional literature, which greatly helped to improve the manuscript. In the following, we provide a point-by-point response to the comments, where comments are in black, and our responses are in blue. In addition, any changes regarding ''author responses to reviewer #2'' applied in the revised manuscript are also colored in blue.

(1) Revised some missing literature (classic and recent) that could impact on the motivation (lines 58-60) and the general definition of the state of the art (lines 28-60). A short list is offered but I suggest expanding it considering the related literature.

Response: We have implemented the suggested literature in the revised manuscript, including Tsang (1992), Brown (1995), Isakov et al. (2001), Ogilvie (2003), Ogilvie et al. (2006), Corradetti et al. (2017), and Zambrano et al. (2019). This work's main goal is to evaluate the reliability of three different methods for the determination of hydraulic aperture and thus fracture permeability. Flow-through experiments can generally provide the most reliable hydraulic results, which we therefore used as a baseline for the comparison with the results obtained by the other two (portable) methods (i.e., the Tiny Perm 3 transient airflow permeameter and a microscope camera-based image analysis). Although fractures can be more precisely characterized using other methods such as surface scans, laser scans, and X-ray computed micro tomography, these methods cannot be employed on a large amount of fractures in outcrop studies. In the present study, our motivation was to investigate how reliably hydraulic fracture properties can be determined under very limited general requirements (e.g., from fracture profiles). In this regard, the ***introduction section*** has been improved by adding the suggested literature and the motivation of the present work was clarified.

(2) Consider revising the grammar and the composition of some sentences that are difficult to understand (e.g. line 23-24).

Response: The manuscript has been checked throughout and revised accordingly.

(3) Concerning the use of the portable permeameter, the discussion and methodological considerations could be improved considering for instance the work of Filomena et al. (2014). These authors found differences of 37% of the permeability measurements between confined and plug samples.

Response: This is a valuable comment. The work by Filomena et al. (2014) is now included and discussed in the manuscript in ***Lines 250-259***.

(4) This work could take benefits of including other approaches for describing roughness and aperture. For instance, evaluating the roughness in terms of wavelength and asperity height distribution can better describe the surfaces (or profiles) of the fractures (see Brown, 1995). In addition, a description of the mismatch of the fracture walls can be also of interest due to their impact of permeability (see Zambrano et al., 2019). Similar to your work, these authors considered open fractures with normal (similar to FF3) and parallel displacement (similar to FOF1 and FF2).

Response: We certainly agree, but the application of the listed other approaches was beyond the scope of this study as outlined in our response to your comment (1) above. Moreover, regarding your second point, a qualitative measure of surface roughness and fracture aperture intensity was used (Fig. 1). For this study, this should prove sufficient because, again, the main goal was to investigate the reliability of different methods for determining the hydraulic aperture of fractures with varying surface roughness and aperture distribution. However, the ***introduction section*** was updated regarding both comments in ***Lines 57-62*** and ***Lines 71-73***.

(5) Concerning the description and the discussion of the results, I consider some statistical validation should accompany some expression like "well-matched", "excellent agreement", "better agreement", "better matching". Also, a better description of the graphs is needed.

Response. We agree. Quantitative statements are now made in ***Lines 301-302*** and ***Lines 316-317***. Moreover, the ***figure captions of Figs. 1, 2, 4, 5, 6, 7, 9, and 11*** were updated.

(6) After all the data exposed, it is difficult to understand the conclusion 3.

Response: We agree and have revised the respective point in the ***conclusions section*** accordingly, highlighted in red (***Lines 389-391***) as this issue was also raised by reviewer #1.

*** *Recommended literature: * ***

Please consider the following classic literature dealing with fracture roughness and hydraulic aperture:

Response: Thank you for the valuable suggestions regarding additional literature. The references colored in blue below were added to the revised manuscript.

- Y. W. Tsang, "Usage of "equivalent apertures" for rock fractures as derived from hydraulic and tracer tests," Water Resources Research, vol. 28, no. 5, pp. 1451–1455, 1992.

- G. M. Lomize, Flow in Fractured Rocks, Gosenergoizdat, Moscow, 1951.

- C. Louis, "A study of ground water flow in jointed rock and its influence on the stability of rock masses," in Rock Mechanics Research Report, Imperial College, London, 1969, Rock Mechanics Research Report 10.

- E. F. de Quadros, Determinação das características do fluxo de água em fraturas derochas, Department of Civil Construction Engineering, Polytechnic School, University of Sao Paulo, 1982.

- S. R. Brown, "Simple mathematical model of a rough fracture," Journal of Geophysical Research: Solid Earth, vol. 100, no. B4, pp. 5941–5952, 1995.

- S. R. Ogilvie, E. Isakov, and P. W. Glover, "Fluid flow through rough fractures in rocks. II: a new matching model for rough rock fractures," Earth and Planetary Science Letters, vol. 241, no. 3-4, pp. 454–465, 2006.

- E. Isakov, S. R. Ogilvie, C. W. Taylor, and P. W. Glover, "Fluid flow through rough fractures in rocks I: high resolution aperture determinations," Earth and Planetary Science Letters, vol. 191, no. 3-4, pp. 267–282, 2001.

- S. R. Ogilvie, E. Isakov, C. W. Taylor, and P. W. J. Glover, "Characterization of rough walled fractures in crystalline rocks," Geological Society, London, Special Publications, vol. 214, no. 1, pp. 125–141, 2003.

Please also add some literature about roughness assessment using SfM photogrammetry and hydraulic aperture estimation using computer fluid dynamics (i.e. Zambrano et al., 2019). The following literature should be considered in paragraph 55:

Response: The suggested references were added to the revised manuscript in ***Line 57***.

- Zambrano, M., Pitts, A. D., Salama, A., Volatili, T., Giorgioni, M., & Tondi, E. (2019). Analysis of Fracture Roughness Control on Permeability Using SfM and Fluid Flow Simulations: Implications for Carbonate Reservoir Characterization. Geofluids.

- Corradetti, A., McCaffrey, K., De Paola, N., & Tavani, S. (2017). Evaluating roughness scaling properties of natural active fault surfaces by means of multi-view photogrammetry. Tectonophysics, 717, 599-606.

Check the classic of Barton et al. (1985) that relate mechanical aperture, hydraulic aperture, and joint roughness coefficient.

Response: The suggested reference was added to the revised manuscript in ***Lines 30-31*** and ***Line 34***.

- Barton, N., Bandis, S., & Bakhtar, K. (1985, June). Strength, deformation and conductivity coupling of rock joints. In International journal of rock mechanics and mining sciences & geomechanics abstracts (Vol. 22, No. 3, pp. 121-140). Pergamon.

Please check carefully the following article related to the use of the miniperm device.

Response: As mentioned in our response to comment (3), the work by Filomena et al. (2014) is now included and discussed in the manuscript in ***Lines 250-259***.

- Filomena, C. M., Hornung, J., & Stollhofen, H. (2014). Assessing accuracy of gas driven permeability measurements: a comparative study of diverse Hassler-cell and probe permeameter devices. Solid Earth, 5(1), 1.

Measuring hydraulic fracture apertures: a comparison of methods

Chaojie Cheng[1,2], Sina Hale[3], Harald Milsch[1], Philipp Blum[3]

[1] GFZ German Research Centre for Geosciences, Section 4.8 Geoenergy, Telegrafenberg, 14473 Potsdam, Germany
[2] University of Potsdam, Institute for Geosciences, Karl-Liebknecht-Str. 24-25, 14476 Potsdam, Germany
5 [3] Karlsruhe Institute of Technology (KIT), Institute of Applied Geosciences (AGW), Adenauerring 20b, 76131 Karlsruhe, Germany

Correspondence to: Harald Milsch (milsch@gfz-potsdam.de)

Abstract. Hydraulic fracture apertures predominantly control fluid transport in fractured rock masses. Hence, the objective of the current study is to investigate and compare three different laboratory scale methods to determine hydraulic apertures in
10 fractured (Fontainebleau and Flechtinger) sandstone samples with negligible matrix permeability. Direct measurements were performed by using a flow-through apparatus and a transient-airflow permeameter. In addition, a microscope camera permitted to measure the mechanical fracture apertures from which the corresponding hydraulic apertures were indirectly derived by applying various empirical correlations. Single fractures in the sample cores were generated artificially either by axial splitting or by a saw cut resulting in hydraulic apertures that ranged between 8 µm and 66 µm. Hydraulic apertures, accurately
15 determined by the flow-through apparatus, are used to compare results obtained by the other methods. The transient-airflow permeameter delivers accurate values, particularly when repeated measurements along the full fracture width are performed. In this case, the derived mean hydraulic fracture apertures are in an excellent quantitative agreement. When hydraulic apertures are calculated indirectly from optically determined mechanical apertures using empirical equations, they show larger variations that are difficult to be compared with the flow-through derived results. Variations in hydraulic apertures as observed between
20 methods are almost certainly related to differences in sampled fracture volume. Overall, using direct flow-through measurements as a reference, this study demonstrates the applicability of portable methods to determine hydraulic fracture apertures at both the laboratory and outcrop scales.

1 Introduction

Rock fracture aperture, allowing for fluid flow, mainly controls the transport properties of rock masses in the subsurface. This
25 quantity is of significant importance for both natural fluid flow within the Earth's crust and geotechnical applications such as oil and gas exploitation in petroleum reservoirs, hydrothermal fluid flow in geothermal systems, CO_2 sequestration, and the underground storage of nuclear waste. Thus, reliable and accurate methods for determining fracture aperture and therefore the permeability of fractured rocks are essential.

The hydraulic aperture, which permits a certain flow rate at a given pressure gradient, represents the capability of fluid flow
30 through a rock fracture. It is typically derived by assuming a parallel plate model (Snow, 1969; Neuzil and Tracy, 1981; Barton

et al., 1985; Tsang, 1992). For the laminar flow of an incompressible Newtonian fluid between two smooth and parallel plates, the flow rate is proportional to the third power of hydraulic aperture, which is commonly referred to as the "cubic law" (Witherspoon et al., 1980). In contrast, the mechanical aperture is defined as the arithmetic average distance between the adjacent fracture walls measured perpendicular to a reference plane (Barton et al., 1985; Hakami and Larsson, 1996; Renshaw et al., 2000). Previously, the relative roughness expressed by the ratio of the standard deviation of the measured mechanical aperture and the mean mechanical aperture was used to estimate hydraulic fracture aperture (Zimmerman et al., 1991; Renshaw, 1995; Barton and de Quadros, 1997; Xiong et al., 2011; Kling et al., 2017). In addition, a correlation between hydraulic and mechanical aperture was established introducing the contact area ratio, defined as the ratio of the true contact area of fracture asperities and the apparent total fracture surface area of a single fracture (Walsh, 1981). The hydraulic aperture of a single fracture can be determined either directly by using the "cubic law" or indirectly based on the mechanical aperture. Typically, the evaluation of the hydraulic aperture is often performed on fractured core samples using flow-through apparatuses at the laboratory scale. Moreover, outcrop studies are widely used to characterize fracture patterns involving, e.g., orientations, distribution, length, and networks within a certain reservoir unit to evaluate its hydraulic performance (Zeeb et al., 2013). The fracture information obtained from outcrops can help define a physical model to understand subsurface fractures (e.g., Bruines, 2003; Watkins et al., 2015; Ukar et al., 2019). Therefore, collecting as much detailed information as possible from the outcrop itself is essential for any further assessment of fracture properties and behaviour. Although the hydraulic apertures measured on outcrops do not directly represent hydraulic fracture properties at depth, they can provide valuable results in this regard. Lately, portable devices such as airflow permeameters, which are easier to use and less costly in comparison to flow-through tests, were developed to investigate both porous rocks and fractures on outcrop profiles (Brown and Smith, 2013). With such devices, large outcrop surfaces as well as anisotropy in a porous rock's transport properties were investigated (Huysmans et al., 2008; Rogiers et al., 2013; 2014). However, the reliability of this approach for natural rough fractures remains to be elucidated since the basic calibration of such measurements is only performed using parallel-plate fractures.

Furthermore, the hydraulic aperture of a fractured rock can also be characterized indirectly by statistical measurements of mechanical aperture such as image analysis of fracture profiles performed by progressively grinding an epoxy resin-fixed sample in pre-defined intervals (e.g., Snow, 1970; Hakami and Larsson, 1996; Konzuk and Kueper, 2004), fracture topography determination using profilometry (e.g., Brown and Scholz, 1985a, b; Matsuki, 1999), X-ray computer tomography (e.g., Kling et al., 2016), structure from motion photogrammetry (e.g., Corradetti et al., 2017; Zambrano et al., 2019), magnetic resonance imaging (e.g., Renshaw et al., 2000), and optical methods applied to rock replicas (e.g., Isakov et al., 2001; Ogilvie et al., 2003; Ogilvie et al., 2006). With known fracture surface topographies and fracture aperture patterns, flow-through properties or hydraulic apertures can be evaluated by numerical fluid flow simulations (e.g., Nemoto et al., 2009; Zambrano et al., 2019) or empirical correlations (e.g., Renshaw, 1995; Kling et al., 2017). All these methods have certain limitations, such as being only applicable within the laboratory scale or requiring open fracture surfaces. Correlations between hydraulic and mechanical apertures were commonly established based on 3D information, providing a valuable understanding of the transport properties of fractures (Renshaw, 1995; Barton and de Quadros, 1997; Xiong et al., 2011; Kling et al., 2017). Nevertheless, outcrop
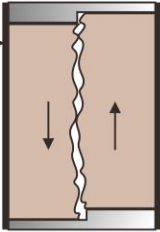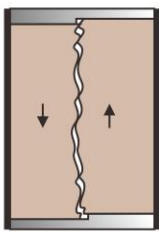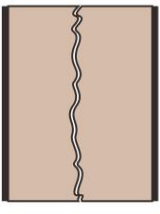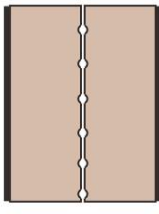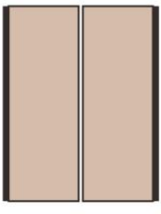
65   studies can only provide single fracture profiles rather than an entire fracture configuration and the question addressed here is whether one can apply these correlations to estimate hydraulic properties based on representative fracture profiles. Accordingly, hydraulic fracture apertures derived by the aforementioned methods have to be compared and evaluated regarding their reliability.

In this study, a systematic comparison of three different methods to determine hydraulic fracture apertures using 1) a flow-

70   through apparatus, 2) a transient-airflow permeameter, and 3) a microscope camera was performed on the same set of sandstone samples to evaluate the reliability, accuracy, and comparability of the results. Natural fractures might appear aligned or mismatched, rough or relatively smooth at different scales, which would affect their hydraulic properties significantly (Barton et al., 1985; Brown, 1995; Zambrano et al., 2019). Thus, the hydraulic aperture was measured on various types of artificially induced single rock fractures, i.e., mismatched rough tensile fractures with defined relative offsets, a matched rough tensile

75   fracture, a saw-cut rough fracture, and a saw-cut smooth fracture. Hence, the purpose of this study is a methodological comparison rather than a study on specific rock types.

2 Materials and methods

2.1 Rock samples

Five cylindrical sandstone core samples, namely Fontainebleau sandstone (e.g., Saadi et al., 2017) (labeled FOF1 and FOF4)

80   and Flechtinger sandstone (e.g., Fischer et al., 2012) (labeled FF2, FF3 and FF4) with 30 mm in diameter and 40 mm in length were prepared for this study. The porosity and the average pore diameter, as determined by mercury intrusion porosimetry, of the present Fontainebleau and Flechtinger sandstones are 2.3 % / 0.7 μm and 9.4 % / 3.8 μm, respectively. Both rocks are characterized by a low matrix permeability in the order of 10^{-18} m^2 as derived from previous measurements (e.g., Blöcher et al., 2009). Single tensile fractures or saw-cut fractures were artificially induced along the sample axis (Fig.1). Tensile fractures

85   in FOF1, FF2 and FF3 were induced using a Brazilian test setup yielding negligible edge damage at a displacement rate of 2 $\times$ 10^{-6} m/s. The separated halves were subsequently assembled with or without installing PEEK gaskets on the top and bottom of the sample to create fixed displacements with pre-offsets of 0.75 mm (FOF1) and 0.20 mm (FF2). The two halves of sample FF3 were matched without offset. Samples FF4 and FOF4 contained a single saw-cut fracture. Due to the larger pore size and higher porosity of Flechtinger sandstone, the fracture roughness of FF4 is significantly higher compared to that of FOF4. A

90   heat-shrink tubing was used to jacket the samples comprising a thin metal sheet placed between the fracture gap and the jacket to minimize a risk of jacket rupture when the sample is under pressure in the flow-through apparatus. For all measurements, the samples were constrained by this heat-shrink tubing ensuring the comparability between methods as the respective fracture configuration was identical in each case.

95

Figure 1: Fracture configurations used in this study and **strategy of sample preparation. The number of stars qualitatively indicates the relative intensity of surface roughness and fracture aperture. The** top **and** bottom **sample surfaces were used for the measurements of the mechanical aperture. a) FOF1, tensile fracture with a pre-offset of 0.75 mm along the sample axis; b) FF2, tensile fracture with a pre-offset of 0.2 mm; c) FF3, matched tensile fracture; d) FF4, saw-cut rough fracture; e) FOF4, saw-cut**

100 **smooth fracture.**

2.2 Experimental methods

As shown in Fig. 2, three different experimental devices were used to investigate the hydraulic aperture of the five samples, namely 1) a flow-through apparatus (FTA; Fig. 1a), 2) a transient-airflow permeameter (TP; Fig. 1b), and 3) a microscope

105 camera (MC; Fig. 1c). All samples were measured with each method in the order of FTA, TP, and MC. A brief outline of the three devices and the respective methods is provided subsequently.
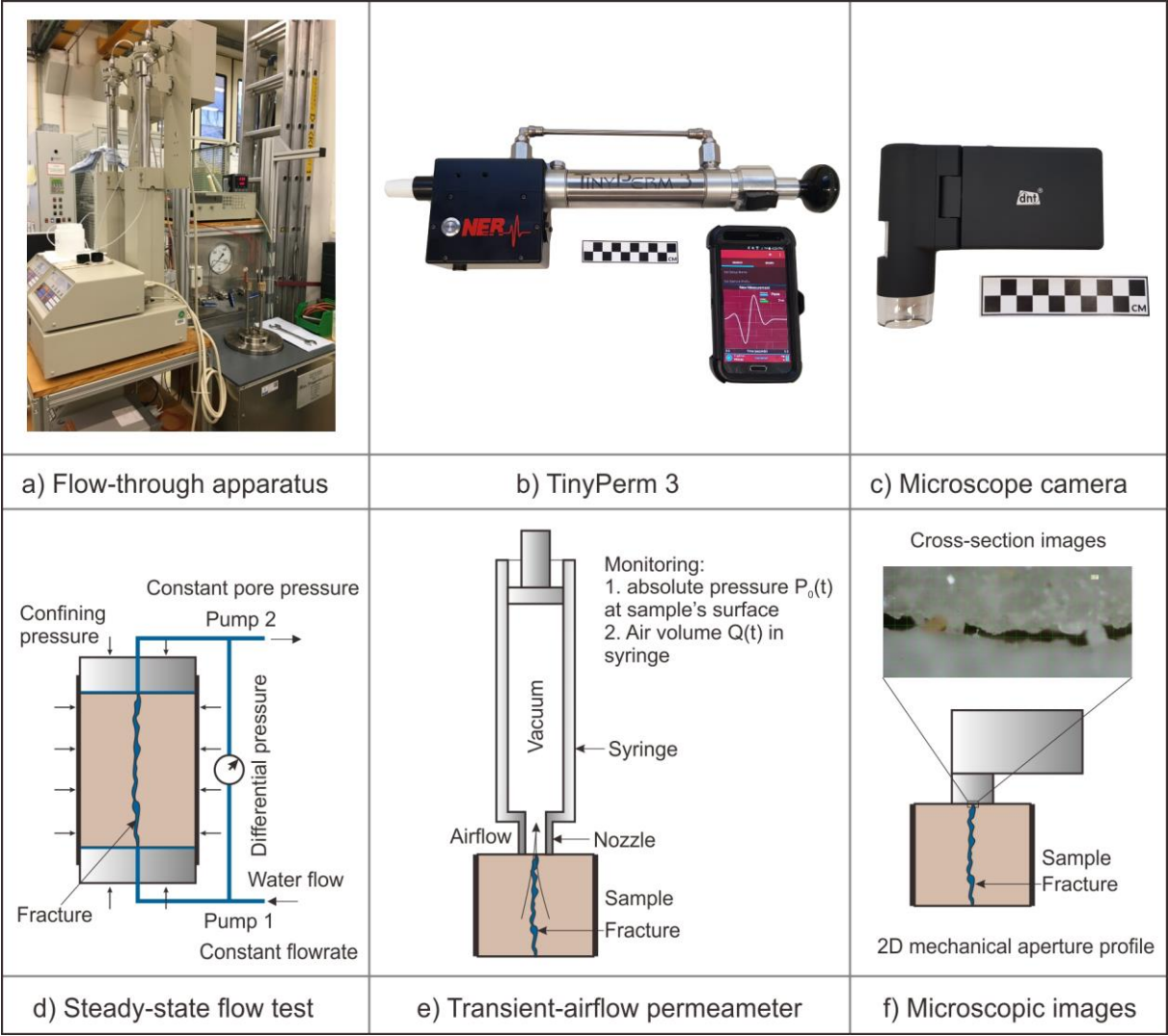
Figure 2: Images of experimental devices a) – c) and illustration of the applied methodology used for hydraulic fracture aperture determination d) – f). a) Flow-through apparatus; b) portable transient-airflow permeameter ("TinyPerm 3"); c) microscope camera; d) steady-state flow test with a) to determine hydraulic aperture based on the "cubic law"; e) hydraulic aperture measured with b) by transient air withdrawal from the rock sample to the vacuum syringe; f) 2D mechanical aperture profile observed with c).

2.2.1 Flow-through apparatus

The absolute liquid (water) permeability of the fractured core samples was measured using a flow-through apparatus (FTA), as shown in Fig. 2a (Milsch et al., 2008), where the jacketed sample core is mounted in a pressure vessel (Fig. 2d). The hydrostatic confining pressure is generated with silicon oil using a syringe pump (ISCO 65D). The pore pressure is controlled by a downstream pump (ISCO 260D) set at constant pressure mode. The upstream pump (ISCO 260D) is connected to the inlet at the lower end of the sample providing a constant fluid flow rate. During a flow-through experiment the pressure

120   difference between the sample ends is monitored by a differential pressure transducer (IPD 40, ICS Schneider Messtechnik) with a measurable range of 0.0-0.6 MPa and an accuracy of < 0.2 %. Deionized water was used as the pore fluid and the permeability of the sample k_{sample} was evaluated using Darcy's Law (Darcy, 1856):

$$k_{sample} = \frac{Q\mu L}{\Delta p \cdot A} \tag{1}$$

where Q, μ, L, Δp are the flow rate, the dynamic fluid viscosity, the sample length, and the differential pressure between the

125   sample ends, respectively. A is the cross-sectional area of the sample. In case the sample permeability is very large compared to the matrix permeability, it is reasonable to assume that the total amount of flow through the sample is equal to the flow through the artificial fracture (Hofmann et al., 2016). Then, based on the "cubic law" and the assumption of laminar flow through the fracture, the fracture permeability can be evaluated from the hydraulic aperture determined by using a parallel-plate approximation (Snow, 1969; Witherspoon et al., 1980; Milsch et al., 2016):

130
$$a_{FTA} = \sqrt[3]{\frac{12Q\mu L}{W \cdot \Delta p}} \tag{2}$$

$$k_f = a_{FTA}^2/12 \tag{3}$$

where W is the fracture width equal to the sample diameter, k_f is the fracture permeability, and a_{FTA} is the hydraulic aperture obtained by the flow-through apparatus. In the following, we will compare a_{FTA} as directly derived from hydraulic measurements with the results obtained by the other two methods.

135

2.2.2 Transient-airflow permeameter

A transient-airflow permeameter (TP; "TinyPerm 3" by New England Research Inc.) was used to independently determine the hydraulic fracture aperture of a sample (Fig. 2b). This portable device can be applied both in the laboratory and the field for direct measurements on core samples and outcrops, respectively. The theory of this device was derived by Brown and Smith

140   (2013) yielding a response function H:

$$H = \frac{\int_{-\infty}^{\infty} Q(t)dt}{\int_{-\infty}^{\infty} P_0(t)dt} \tag{4}$$

where $Q(t)$ is the flow profile and $P_0(t)$ is the pressure profile through time measured by the instrument's pressure transducer and flowmeters. Figure 2e shows the measurement principle. By pushing down the piston to create a vacuum within the chamber, air starts to flow from the sample to the syringe through the nozzle tip, ultimately re-establishing atmospheric

145   pressure conditions therein. Consequently, two time-dependent profiles $Q(t)$ and $P_0(t)$ can be obtained. It should be noted that the measured response function H is strongly related to the sample permeability and that other parameters, such as the geometry of the rock specimen, are also needed to ultimately determine permeability. Some of these parameters may be difficult to obtain, especially in the field. Thus, an empirical calibration of the device was conducted with an artificial fracture

consisting of two polished granite samples whose aperture can be controlled by the thickness of feeler gauges in between,

150   yielding (Brown and Smith, 2013):

$$T = -1.5 \log_{10}(a_{TP}) + 8.29 \tag{5}$$

where a_{TP} is the hydraulic fracture aperture, which is assumed equivalent to the known separation (i.e., the mechanical aperture) of the parallel granite plates, and T is a value obtained from a measurement with the TP, which is the common logarithm of the final H when the pressure in the syringe returns to ambient pressure. Based on this empirical calibration and by directly

155   measuring the response function H, hydraulic fracture apertures can be determined with this device (New England Research, 2015). The validity of this method was tested on parallel-plate fractures in the range between 20 µm and 2 mm, yielding a insignificantly small uncertainty of ± 1.4% (Brown and Smith, 2013). Nevertheless, for natural rough fractures, to our knowledge, no validation and also no precision assessment have been performed yet. Based on measurements with this device, we will demonstrate its reliability for applications on natural fractures.

160   **2.2.3 Microscope camera**

Mechanical aperture can be determined by measuring the vertical distances between the upper and lower fracture walls perpendicular to a predefined global reference plane (Hakami and Larsson, 1996) or by measuring the separation distances oriented perpendicular to the local trend of the fracture walls (Mourzenko et al., 1995; Ge, 1997) as illustrated in Fig. 3. Konzuk and Kueper (2004) compared the two methods with the same fracture aperture revealing that the mean local perpendicular

165   aperture is about 8% smaller than the mean global vertical aperture, while their aperture histograms essentially yield similar shape.

In this study, due to the fact that the microscopic images only represent small segments of the fracture in a sample, one cannot unequivocally define a global reference plane that would fit all images. Therefore, an estimation of the local perpendicular distance between the adjacent fracture walls was used to maintain consistency in the analysis between individual images. 2D

170   aperture profiles were manually obtained at the sample end faces (Fig. 2c, f) using a microscope camera (MC; DigiMicro Mobile, dnt GmbH). Applying the software "PortableCapture", the perpendicular distance a_i (Fig. 3) between the captured fracture edges was measured at 20 equidistant spots on the picture defined by a mesh grid. Knowing the magnification factor of the microscope camera, the true distance between the fracture walls can be calculated for each spot. The magnification factors ranged between 200 and 206, corresponding to an investigated area of 1.72×2.29 mm^2 to 1.67×2.23 mm^2, respectively.

175   More details can be found in (Hale et al., 2019). The mechanical fracture aperture a_m corresponds to the arithmetic mean of the measured distances in each image and was calculated by:

$$a_m = \frac{1}{n} \sum_{i=1}^{n} a_i \tag{6}$$
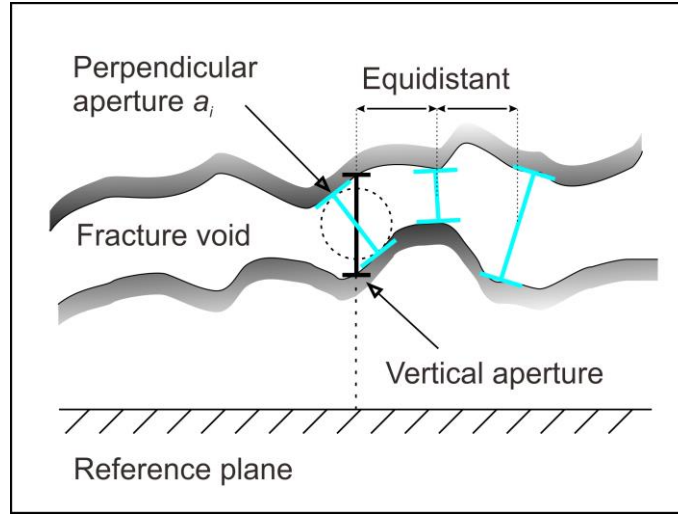
Figure 3: Conceptual illustration of different mechanical aperture definitions and the estimation method applied in this study (indicated in blue); modified from Konzuk and Kueper (2004).

Empirical equations based on a_m and the standard deviation of measured aperture values σ_a were subsequently used to estimate the hydraulic aperture a_h (Table 1).

Table 1. Summary of empirical equations used to estimate hydraulic fracture apertures from measured mechanical apertures.

No.	Equation	Fracture type	Reference
1	$a_h \approx a_m \left(1 + \dfrac{\sigma_a^2}{a_m^2}\right)^{-\frac{1}{2}}$	Theoretical equation based on stochastics for lognormal aperture distribution	Renshaw (1995)
2	$a_h \approx \dfrac{a_m}{\sqrt[3]{1 + 20.5 \left(\dfrac{\sigma_a}{2a_m}\right)^{\frac{3}{2}}}}$	Natural granite fractures	Barton and de Quadros (1997)
3	$a_h \approx a_m \cdot \sqrt[3]{1 - \dfrac{1.13}{1 + 0.191 \left(\dfrac{2a_m}{\sigma_a}\right)^{1.93}}}$	Tensile granite fracture	Matsuki (1999)
4	$a_h \approx a_m \cdot \sqrt[3]{1 - \dfrac{\sigma_a}{a_m}}, \ \ \dfrac{\sigma_a}{a_m} < 1$	Replicas of a split sandstone and natural granite fracture	Xiong et al. (2011)
5	$a_h \approx a_m \cdot \left(1 + \dfrac{\sigma_a}{a_m}\right)^{-\frac{3}{2}}$	Numerical model of fracture sealing by hydrothermally grown quartz	Kling et al. (2017)

Note: a_h is estimated based on the relative roughness of a fracture, which can be expressed as the ratio between the standard deviation σ_a and the corresponding arithmetic mean mechanical aperture a_m.

Based on the analysis of all microscopic images for each sample, the mechanical aperture distribution can additionally be determined. As the minimum measurable distance was limited to 10 μm, one can apply a threshold of 10 μm, where mechanical apertures smaller than the threshold are considered as contacting asperities (Hakami and Larsson, 1996). Consequently, the contact area ratio R_c can be derived by quantifying the ratio of the number of contacting asperities and the total number of a_i. By assuming circular contact areas of the asperities oriented in parallel to the fracture plane, a hydraulic aperture a_H can be obtained from the total mean mechanical aperture and R_c as follows (Walsh, 1981; Zimmerman et al., 1992):

$$a_H^3 = \frac{1-R_c}{1+R_c} a_m^3 \tag{7}$$

2.3 Experimental procedures

For the flow-through experiments the assembled rock samples were vacuum-saturated with deionized water in a desiccator. The specimen assembly was mounted in the pressure vessel of the FTA for the permeability measurements. The confining pressure was first increased to 4 MPa and, subsequently, the pore pressure was increased to 1 MPa and maintained constant throughout the measurement. The confining pressure was then increased to 5 MPa, implying that the effective pressure applied to the sample was 4 MPa as the starting condition. It is well known that a first loading ramp causes the largest irreversible aperture closure as compared to further loading-unloading sequences (Hofmann et al., 2016; Milsch et al., 2016). In this study, one confining pressure loading-unloading cycle from 5 MPa to 30 MPa and back to 5 MPa (FOF1) or 2 MPa (FOF4, FF2, FF3, and FF4) was performed at room temperature. The sample permeability was measured at each pressure step in defined confining pressure intervals. Due to the fact that the samples were subject to near-zero effective pressure when applying the other two methods (TP and MC), the hydraulic apertures at zero effective pressure were obtained from curve-fitting of the measured data during unloading (Sect. 3.1; Fig. 4) and used for comparison.

After completion of the flow-through experiment, the respective specimen assembly was removed from the pressure vessel. The plugs and gaskets were taken off to expose the end faces of the samples for the subsequent TP measurements. The heat-shrink tubing, however, was kept in place in order to fasten the two halves of the specimen. The samples were then dried in an oven at 60 °C for several days to obtain defined test conditions for the TP measurements. The hydraulic fracture aperture a_{TP} was finally measured with the TP at ambient pressure and temperature conditions. Since the inner diameter of the TP's rubber nozzle is 8 mm and the diameter of the core was 30 mm, the effective cross-sectional area for the airflow is significantly smaller than the total cross-sectional area of the core sample as investigated in the flow-through experiments. Thus, the hydraulic aperture was measured ten times on both the top and bottom end faces of the sample in order to fully cover the fracture across the sample diameter. Care needs to be taken as, unlike for fractures between adjacent parallel plates, gas might slip asymmetrically from the fracture at the end of the nozzle due to the irregular fracture void space. Single measurements at

different sites on the same sample end may lead to discrepancies. Therefore, multiple measurements are essential when applying the TP on rough fractures.

Finally, mechanical aperture profiles on both sample end faces were determined with the MC. 13 to 17 images were taken on each surface, namely 26 to 29 images in total for each sample, to fully cover the aperture profile across the sample diameter. It should be recalled that all samples were tested by TP and MC after the flow-through experiments (FTA) yielding identical fracture configurations and nearly identical measurement conditions for evaluating the hydraulic apertures determined by the three methods.

3 Results and discussion

In the following two sub-sections the hydraulic aperture data as determined in this study is presented (Section 3.1) and compared among measurement methods (Section 3.2). All data related to this publication are attached as Supplementary Material.

3.1 Measured hydraulic fracture apertures

The FTA experiments and the TP measurements represent direct methods for determining hydraulic fracture aperture. Figure 4 shows the hydraulic apertures measured with the FTA (a_{FTA}) at different effective pressures during unloading. Subsequently, the hydraulic apertures at zero effective pressure were predicted by extrapolation of the different unloading sequences, yielding 65.9 µm for FOF1, 37.0 µm for FF2, 9.8 µm for FF3, 47.6 µm for FF4, and 7.7 µm for FOF4, respectively. The mismatched rough fractures (FOF1 and FF2) and the saw-cut rough fracture (FF4) are characterized by relatively large hydraulic apertures, whereas the matched rough fracture (FF3) and the saw-cut smooth fracture (FOF4) yield significantly smaller and nearly identical hydraulic apertures.
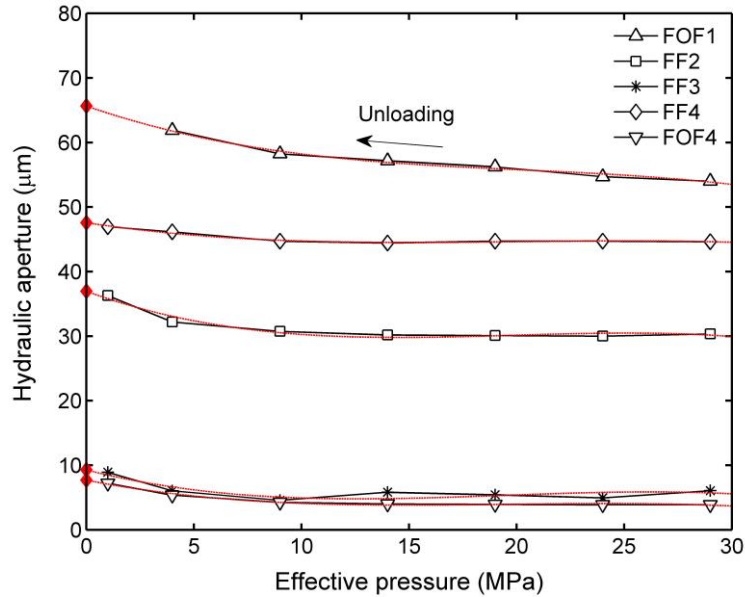
Figure 4: Hydraulic aperture a_{FTA} (obtained by the flow-through apparatus) as a function of effective pressure during unloading. Each point is a steady-state permeability measurement at the respective effective pressure. The fitted curves (red lines) represent the hydraulic aperture of each fractured sample at zero effective pressure (red diamonds).

Figure 5 shows the hydraulic apertures a_{TP} determined with the TP, where the results show higher variability for the samples with larger apertures (FOF1, FF2, and FF4) in contrast to the samples with smaller apertures (FF3 and FOF4). Since the nozzle of the TP is smaller in size than the cross-sectional area of the present core samples, the individually measured hydraulic aperture values do not necessarily represent the hydraulic aperture of the entire sample. On the other hand, due to the roughness of the fracture profile, airflow from the fracture to the nozzle might be largely asymmetric, particularly close to the fracture edge. This is possibly the reason for large variations in case of larger fractures. Therefore, the range of the hydraulic aperture values of each sample can serve as an indicator for the variability of the hydraulic aperture along the fracture width. Samples FF3 and FOF4 only show insignificant variations resulting from the matched and smooth surfaces, respectively, indicating a rather constant aperture across the samples. Previously, Filomena et al. (2014) demonstrated a sample size effect for permeability measurements using the TP device on 1-inch core samples (i.e., porous media without fractures). As core sample permeabilities were about 37% larger than permeabilities measured on corresponding block samples, they concluded that the discrepancy is mainly due to the effect of shorter flow trajectories in core samples. However, this is not the case for our fractured samples. Firstly, it is impossible to perform fracture permeability measurements at the core sample scale without any constraints. Therefore, all samples were jacketed with a heat-shrink tubing to maintain the fracture patterns. Secondly, when performing TP measurements on fractured core samples, the samples' jacket limits the leakage of the flow from the fracture

edges. Thus, the obtained results are in good agreement with the hydraulic apertures determined by the flow-through experiments (Section 3.2). For measuring larger fracture profiles in block samples (e.g., Hale et al., 2019) or outcrops, this would not be an issue since the flow trajectories are sufficiently long.

260
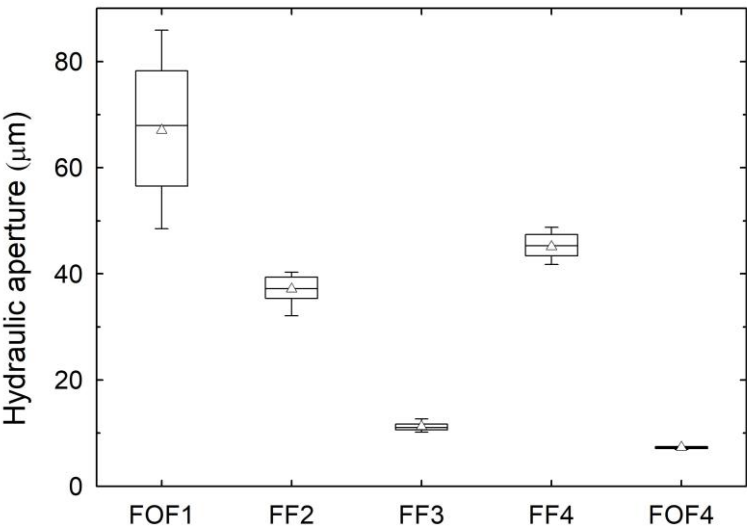
Figure 5: Hydraulic fracture aperture of each sample measured with the transient-airflow permeameter (TP), including a total of 20 values for each sample taken at the top and bottom end faces (see Fig. 1). The solid line and the open triangle in the box indicate the median and mean of each dataset, respectively.

265

Figure 6 shows representative microscopic images of the fractures taken with the MC. The 2D mechanical aperture a_m in each image was measured by determining the distance between the upper and lower fracture wall at 20 evenly spaced spots. The arithmetic mean of the measured distances in each image was subsequently calculated representing the mean mechanical fracture aperture of the observed area. The mechanical apertures derived from all profile images of each sample are shown in

270 Fig. 7, yielding significantly larger variations in aperture values in comparison to the corresponding TP hydraulic apertures a_{TP} (Fig. 5).
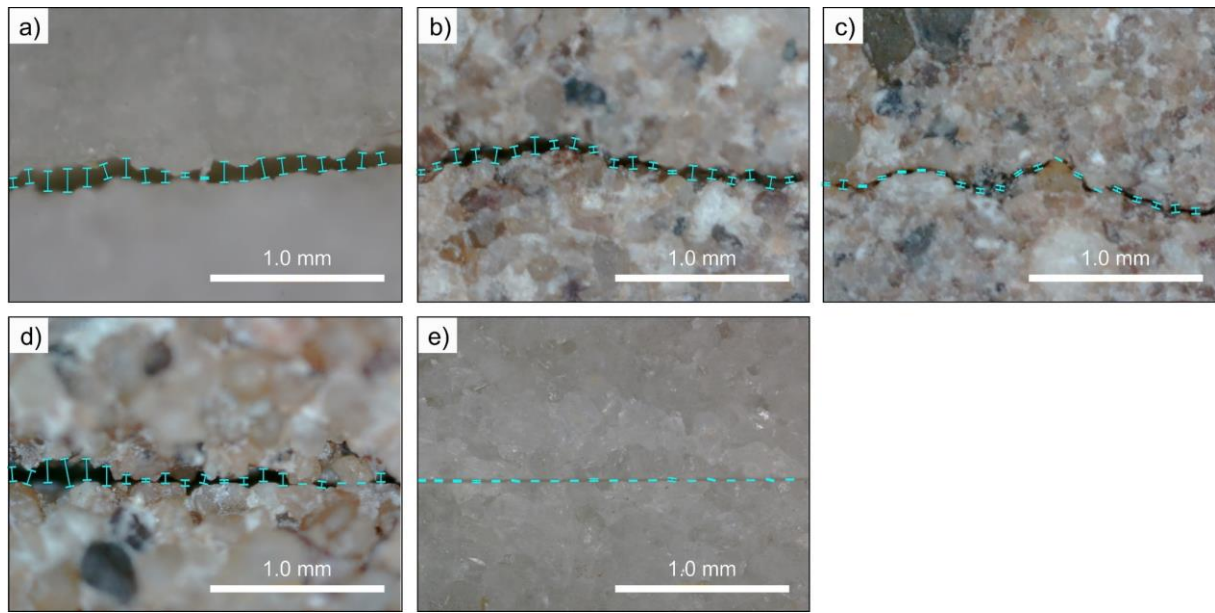
Figure 6: Representative microscopic images of the samples comprising parts of the respective fracture profiles. a) FOF1, with a pre-offset of 0.75 mm; b) FF2, with a pre-offset of 0.2 mm; c) FF3, matched rough fracture; d) FF4, saw-cut rough fracture; e) FOF4, saw-cut smooth fracture. The distances between the upper and lower fracture walls were measured at equidistant locations.
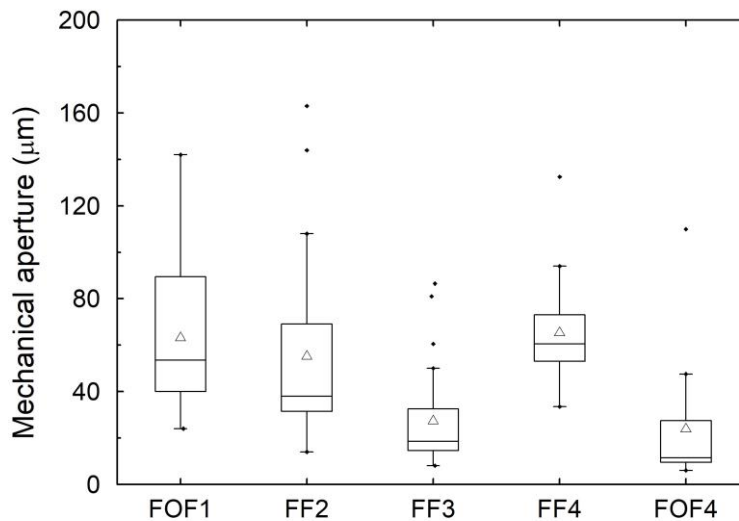
Figure 7: Mechanical apertures of the samples derived from image series taken on the top and bottom end faces with the microscope camera (MC). Individual symbols (black dots) above the whiskers represent measured data but are statistical outliers. In the box plots, the boxes signify the lower and upper quartiles (Q1 and Q3) of the data sets, respectively. The upper and lower whiskers indicate the largest and smallest data values for Q3 + 1.5 IQR and Q1 - 1.5 IQR, respectively, where IQR is the interquartile range equal to Q3 - Q1. The solid line and the open triangle in the box indicate the median and mean of each dataset, respectively.

285 From the totality of measured distances based on all 2D microscope images of each sample, their respective mechanical aperture distributions can be derived as shown in Fig. 8. The contact area ratio R_c of samples FOF1, FF2, FF3, FF4, and FOF4 is 0.142, 0.173, 0.186, 0.054, and 0.150, respectively, as resulting from the loading-unloading cycle in the FTA. As expected, the matched fracture surfaces of FF3 exhibit the largest contact area ratio compared to all other samples. The hydraulic aperture a_H can be subsequently derived with Eq. (7) using the corresponding total mean mechanical aperture as well as R_c. The

290 resulting hydraulic apertures of FOF1, FF2, FF3, FF4, and FOF4 are 57.4 µm, 49.1 µm, 24.1 µm, 63.0 µm, and 21.5 µm, respectively. Based on the former total mean mechanical apertures and their standard deviations, hydraulic apertures were additionally evaluated using the empirical equations listed in Table 1 as outlined and discussed in Sect. 3.2 below.
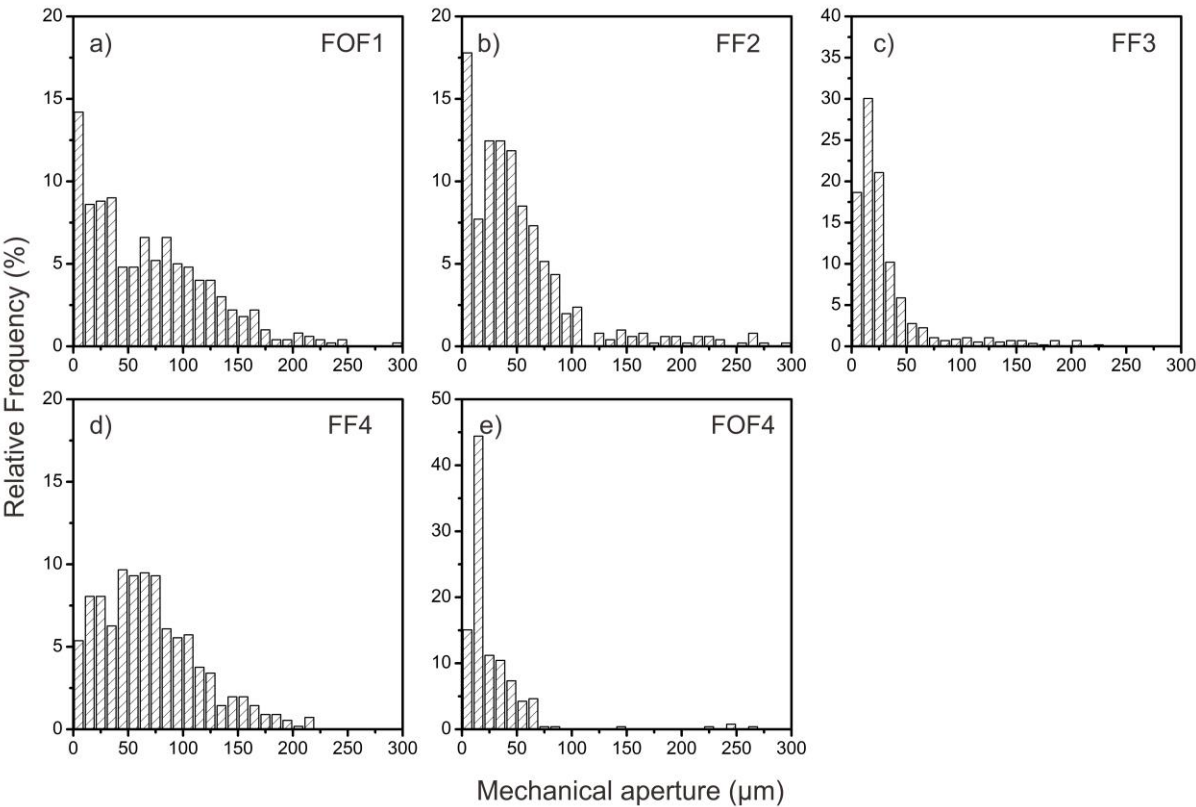
295 **Figure 8: Frequency histograms showing the mechanical aperture distribution obtained from the 2D microscopic images of each sample. a) FOF1; b) FF2; c) FF3; d) FF4; e) FOF4.**

3.2 Comparison of hydraulic fracture apertures

Figure 9 presents an overall comparison of hydraulic apertures of all samples measured with the FTA, the TP, and the MC.

300 The mean and median hydraulic apertures a_{TP} determined with the transient-airflow permeameter are very consistent with the

absolute hydraulic apertures a_{FTA} determined by the flow-through experiments. The differences range between 0.2 µm (sample FF2) and 2.5 µm (sample FF4). Furthermore, it can also be seen from this figure that the smaller the hydraulic aperture, the smaller the range of variations. For all samples, the hydraulic apertures a_h derived from the empirical equations listed in Table 1 using the mean mechanical aperture and the corresponding standard deviation from each microscopic image show larger

305 variations in comparison to the hydraulic apertures measured with both the FTA and the TP. This is likely due to the fact that for each individual microscopic image only a 2.29 mm wide part of the fracture was considered, which does not represent the studied fracture over its entire width.
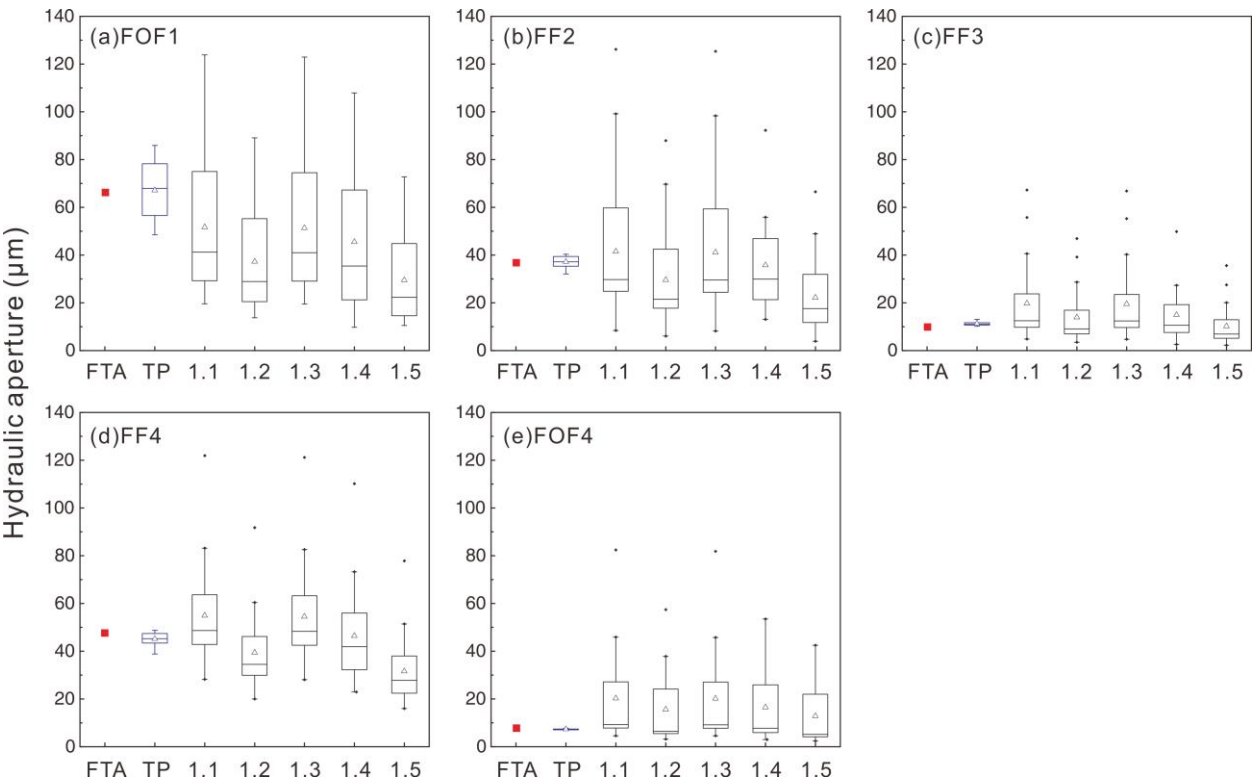
310 **Figure 9: Comparison of hydraulic apertures measured with the flow-through apparatus (FTA; red squares), the transient-airflow permeameter (TP; blue box plot), and derived from MC-measured mechanical apertures (1.1 to 1.5; black box plots) using the empirical equations 1 to 5 listed in Table 1. Individual symbols (black dots) above the whiskers are calculated data but represent statistical outliers.**

315 Figure 10 shows the correlation between the hydraulic apertures a_{TP} measured with the TP and a_{FTA} obtained by the FTA. For each sample, the mean and median values of the TP measurements are in excellent agreement (coefficient of determination R^2 = 0.998) with the ones measured with the FTA. It is noted that all measured a_{TP} of sample FF3 are slightly larger than the determined a_{FTA}. Due to the well-matched rough fracture surfaces of FF3, the fracture aperture is significantly smaller in comparison to the other samples (except FOF4). Hence, already a small applied stress may result in a comparatively significant

aperture decrease and the predicted zero-stress aperture a_{FTA} of FF3 might therefore be slightly underestimated. However, this small discrepancy should be acceptable when the TP is applied in the field. Based on this comparison with samples under unstressed conditions, one can infer that measurements with both FTA and TP would yield an even better agreement when hydraulic apertures are determined at elevated stress conditions. This is because the geometric stability of fracture aperture increases as the normal stress on a fracture plane increases (e.g., Fig. 4). In addition, the standard deviations σ_a of the hydraulic apertures a_{TP} of samples FOF1, FF2, FF3, FF4, and FOF4 are 12.0 µm, 2.3 µm, 0.9 µm, 2.6 µm, and 0.3 µm, respectively, which clearly demonstrates that for smaller hydraulic apertures less variability of measured values can be observed.

As mentioned before, for TP measurements of hydraulic aperture (a_{TP}), the effective sampled area of the rubber nozzle in contact with the sample surface is smaller than the sample's cross-sectional area. Consequently, the results, particularly for samples with a larger hydraulic aperture, show substantial variations. However, by conducting multiple measurements to fully cover the entire cross-sectional area, the mean and median hydraulic aperture a_{TP} and the corresponding absolute hydraulic aperture a_{FTA} showed an excellent agreement. The investigation depth of the transient-airflow permeameter for isotropic porous media was estimated to be approximately twice the internal radius of the nozzle tip (Goggin et al., 1988; Jensen et al., 1994; Possemiers et al., 2012) since the largest pressure gradient along a sample occurs near the injection/extraction region. This implies that a certain minimum sample length (i.e., twice the internal radius of the nozzle tip) is required for a reliable permeability measurement. However, for fractures, this minimum length has not been established yet. As mentioned before, the calibration of the TP was performed by using parallel plates as idealized fractures. Increasing the fracture length has no effect on this idealized aperture while a minimum length of the fracture might be required for sufficient airflow. As the length of the measured core samples was 40 mm (i.e., ten times the nozzle tip radius), the total fracture volume was only partially covered during a TP measurement provided that the investigation depth in single fractures is comparable to the one in porous media. Overall, the accuracy and the reliability of hydraulic aperture results obtained from TP measurements can be significantly improved by performing repeated measurements along the fracture width as well as a subsequent statistical evaluation. Nevertheless, a rough fracture in a core longer than 40 mm may lead to less conformity of a_{FTA} and a_{TP} since the transient airflow does not fully cover the entire fracture area.
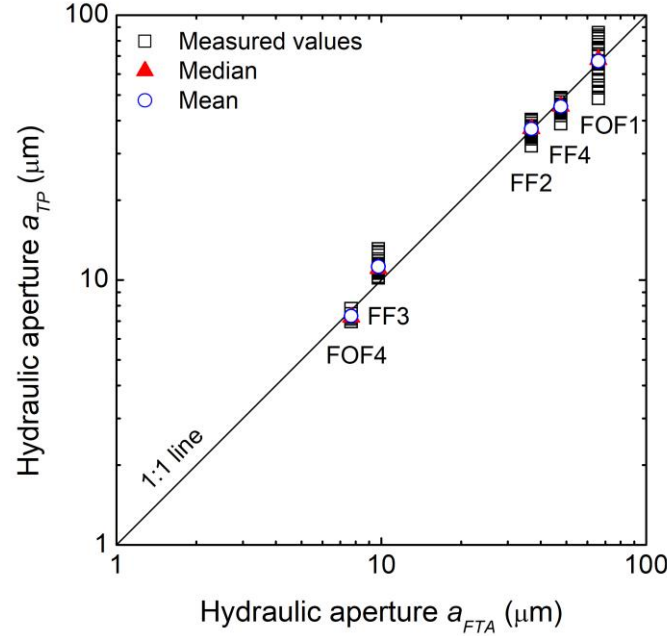
345 **Figure 10: Cross-plot of the hydraulic apertures a_{TP} determined with the transient-airflow permeameter (TP) and the hydraulic apertures a_{FTA} measured with the flow-through apparatus (FTA).**

Figure 11 shows the correlations between the hydraulic aperture a_{FTA} (FTA) and the median (a) and mean (b) hydraulic apertures a_h derived from measured mechanical apertures (MC) when applying the empirical equations listed in Table 1. For

350 the relatively narrow fractures in FOF4 and FF3 with hydraulic apertures around 10 μm, the median of a_h does replicate the actual hydraulic aperture obtained from the flow-through experiments very well, especially when using the equations of Barton and de Quadros (1997) and Xiong et al. (2011). In contrast, the mean of a_h overestimates the respective FTA hydraulic aperture. For the relatively open fractures in FOF1, FF2, and FF4 with hydraulic apertures larger than 30 μm, the arithmetic mean is in better agreement with the respective FTA hydraulic aperture. Overall, it can be concluded that the equations of Barton and de

355 Quadros (1997) and Xiong et al. (2011) yield better matching results for the studied samples as compared to the other equations listed in Table 1.

When additionally deriving the contact area ratio from all images of each sample, Eq. (7) can be applied and compared to the results of hydraulic apertures as calculated using the empirical equations in Table 1 (Fig. 11 c). For samples with hydraulic apertures smaller than 10 μm, the derived results overestimate the actual aperture (a_{FTA}) except for Kling et al. (2017). For

360 hydraulic apertures larger than 30 μm, the derived results almost exclusively underestimate the true values with the exception of those obtained from Eq. (7). Possible errors regarding the input data may be related to the size limit of each microscopic image, where the obtained data can only represent the fracture aperture within the individually observed area with a segment

width of 2.29 mm. Also, since the mechanical aperture distribution and the contact area ratio are obtained from 2D images of the fracture profiles, these do not fully represent the true fracture aperture distribution and contact area ratio in 3D.

365 Nevertheless, the hydraulic apertures of the different samples as derived from the same respective equation are comparable and reflect the relative aperture differences.
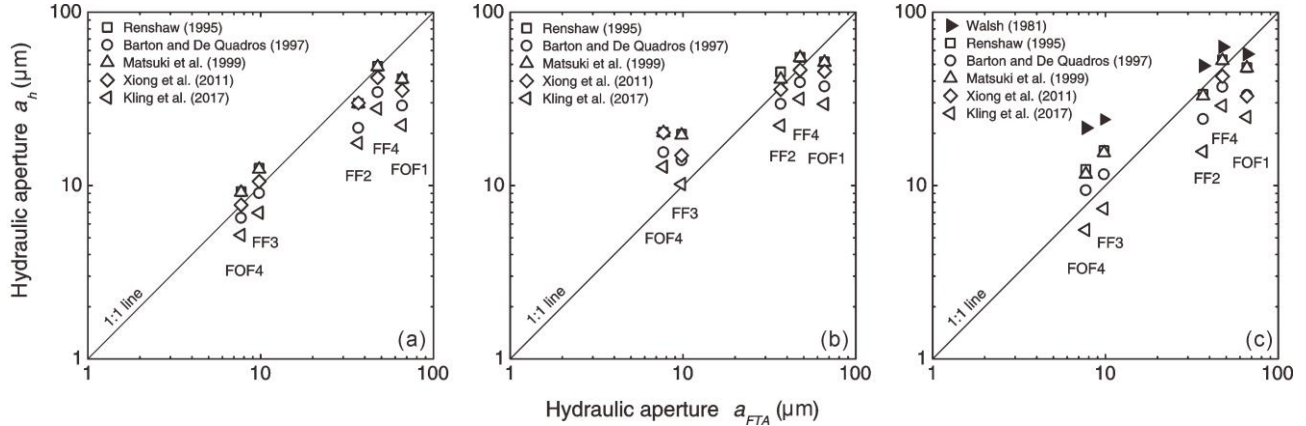
Figure 11: Cross-plots of calculated hydraulic apertures based on microscopic images of fracture profiles (a_h) and hydraulic
370 **apertures a_{FTA} measured with the flow-through apparatus (FTA). a) Median and b) mean hydraulic apertures a_h using MC-based mechanical apertures of each image in combination with the equations listed in Table 1. c) Hydraulic apertures a_H derived from Eq. (7) (black triangles) and hydraulic apertures a_h derived from the totality of measured mechanical apertures of each sample (see Figure 8) are shown for comparison.**

4 Conclusions

375 Three different methodological approaches for hydraulic fracture aperture determination, i.e., using a flow-through apparatus (FTA), a transient-airflow permeameter (TP), and a digital microscope camera (MC), were applied and compared. A total of five (Fontainebleau and Flechtinger) sandstone samples containing single fractures of different types and representing a hydraulic aperture range between 8 μm and 66 μm were investigated. The comparison of the results aimed at assessing the applicability, reliability, and accuracy of each method yielding the following conclusions:

380   1. The agreement of the mean hydraulic apertures determined with the transient-airflow permeameter (a_{TP}) and the corresponding hydraulic apertures measured by flow-through experiments (a_{FTA}) was excellent for all samples.

    2. For rough fractures with hydraulic apertures larger than 30 μm, measurements with the transient-airflow permeameter have to be repeated across the full fracture width in order to statistically obtain reliable results. The investigations additionally showed that this permeameter can also be reliably used to determine hydraulic fracture apertures as small
385   as approximately 5 μm.

    3. The hydraulic apertures estimated by evaluating 2D mechanical aperture profiles in digital microscope camera images showed large variations for all samples and therefore cannot be directly compared to the results obtained by the two other approaches. On the other hand, when applying empirical equations taken from literature, the mean and median

hydraulic apertures derived from the respective correlation, only reflect the relative aperture differences between the fracture types. This approach, consequently, is less useful for any further analysis in comparison to the direct measurements.

In summary, hydraulic fracture apertures can be measured directly and precisely, also as a function of pressure by performing flow-through experiments in appropriate apparatuses. For a large number of routine measurements at ambient conditions this procedure, however, is time-consuming and costly. For such purposes, this laboratory study shows that the transient-airflow permeameter offers a fast and highly efficient approach for hydraulic aperture determination on fracture profiles of cores and probably on outcrops. Multiple measurements around a sampling point can significantly increase the reliability of the results. For the first time this study quantitatively evaluated the reliability and precision of transient-airflow permeameter measurements on natural rough fractures extending previous calibrations based on ideal parallel plates (Brown and Smith, 2013). When following an optical approach using a digital microscope camera, qualitatively correct estimates of hydraulic aperture variations both along a fracture and between different fracture types are obtained. Although conclusions here are drawn from laboratory scale measurements on core samples, these should also be valid when applying the portable methods (TP and MC) on fractures displaying the same aperture range at the outcrop scale. Hence, integrating the results of hydraulic aperture measurements on fractures, both, from core samples and outcrops applying multiple methods will improve our understanding of permeability in fractured rock. However, it should be noted that the conclusions drawn from this study are strictly only valid for the environmental conditions applied (i.e., stress and temperature). Consequently, characterizing the hydraulic aperture of fractures at depth from measurements taken at the surface of an outcrop demands information on the mechanical response of a fracture to stress and temperature. This extrapolation will require the continued application of flow-through devices like the one used in this study and measurements of the type displayed in Fig. 4.

Author contributions

CC prepared all rock samples and performed the experiments with the FTA. SH conducted the TP and MC measurements on the same specimens. All authors (CC, SH, HM, and PB) analyzed and interpreted the results and contributed to drafting the manuscript.

Competing interests

The authors have no competing interests to declare.

Data availability

All data related to this manuscript is attached as Supplementary Material.

Acknowledgments

The authors thank Christian Kluge and Michael Naumann (GFZ Potsdam) for technical support during sample preparation. Chaojie Cheng acknowledges funding by the China Scholarship Council (CSC) under grant No. 201606410056. Financial support by the German Federal Ministry of Education and Research (BMBF) under grant No. 03G0871D, as part of the ResKin (Reaction Kinetics in Reservoir Rocks) project, is also gratefully acknowledged. Constructive reviews by Marco Antonellini and Miller Zambrano are greatly acknowledged and helped to improve this paper.

References

Barton, N., Bandis, S., and Bakhtar, K.: Strength, deformation and conductivity coupling of rock joints, Int. J. Rock Mech. Min. Sci. & Geomech. Abstr., 22, 121-140, doi: 10.1016/0148-9062(85)93227-9, 1985.

Barton, N. and de Quadros, E. F.: Joint aperture and roughness in the prediction of flow and groutability of rock masses, Int. J. Rock Mech. Min. Sci., 34, 252.e1-252.e14, doi: 10.1016/S1365-1609(97)00081-6, 1997.

Blöcher, G., Zimmermann, G., and Milsch, H.: Impact of poroelastic response of sandstones on geothermal power production, Pure Appl. Geophys., 166, 1107-1123, doi: 10.1007/s00024-009-0475-4, 2009.

Brown, S. and Smith, M.: A transient-flow syringe air permeameter, Geophysics, 78, D307-D313, doi: 10.1190/Geo2012-0534.1, 2013.

Brown, S. R. and Scholz, C. H.: Closure of random elastic surfaces in contact, J. Geophys. Res., 90, 5531-5545, doi: 10.1029/JB090iB07p05531, 1985a.

Brown, S. R. and Scholz, C. H.: Broad bandwidth study of the topography of natural rock surfaces, J. Geophys. Res., 90, 12575-12582, doi: 10.1029/JB090iB14p12575, 1985b.

Brown, S. R.: Simple mathematical model of a rough fracture, J. Geophys. Res.-Sol. Ea., 100, 5941-5952, doi: 10.1029/94jb03262, 1995.

Bruines, P.: Laminar ground water flow through stochastic channel networks in rock, Doctoral dissertation, EPFL, Lausanne, 2003.

Corradetti, A., McCaffrey, K., De Paola, N., and Tavani, S.: Evaluating roughness scaling properties of natural active fault surfaces by means of multi-view photogrammetry, Tectonophysics, 717, 599-606, doi: 10.1016/j.tecto.2017.08.023, 2017.

Darcy, H.: Les fontaines publique de la ville de Dijon, Dalmont, Paris, 1856.

Filomena, C., Hornung, J., and Stollhofen, H.: Assessing accuracy of gas-driven permeability measurements: a comparative study of diverse Hassler-cell and probe permeameter devices, Sol. Ea., 5, 1-11, doi: 10.5194/se-5-1-2014, 2014.

Fischer, C., Dunkl, I., von Eynatten, H., Wijbrans, J. R., and Gaupp, R.: Products and timing of diagenetic processes in Upper Rotliegend sandstones from Bebertal (North German Basin, Parchim Formation, Flechtingen High, Germany), Geol. Mag., 149, 827-840, doi: 10.1017/S0016756811001087, 2012.

450 Ge, S.: A governing equation for fluid flow in rough fractures, Water Resour. Res., 33, 53-61, doi: 10.1029/96WR02588, 1997.

Goggin, D., Chandler, M., Kocurek, G. t., and Lake, L.: Patterns of permeability in eolian deposits: Page Sandstone (Jurassic), northeastern Arizona, SPE Format. Evalu., 3, 297-306, doi: 10.2118/14893-PA, 1988.

Hakami, E. and Larsson, E.: Aperture measurements and flow experiments on a single natural fracture, Int. J. Rock Mech.
455   Min. Sci. & Geomech. Abstr., 33, 395-404, doi: 10.1016/0148-9062(95)00070-4, 1996.

Hale, S., Naab, C., Butscher, C., and Blum, P.: Method comparison to determine hydraulic apertures of natural fractures, Rock Mech. Rock Eng., 53, 1467-1476, doi: 10.1007/s00603-019-01966-7, 2019.

Hofmann, H., Blocher, G., Milsch, H., Babadagli, T., and Zimmermann, G.: Transmissivity of aligned and displaced tensile fractures in granitic rocks during cyclic loading, Int. J. Rock Mech. Min. Sci., 87, 69-84, doi:
460   10.1016/j.ijrmms.2016.05.011, 2016.

Huysmans, M., Peeters, L., Moermans, G., and Dassargues, A.: Relating small-scale sedimentary structures and permeability in a cross-bedded aquifer, J. Hydrol., 361, 41-51, doi: 10.1016/j.jhydrol.2008.07.047, 2008.

Isakov, E., Ogilvie, S. R., Taylor, C. W., and Glover, P. W.: Fluid flow through rough fractures in rocks I: high resolution aperture determinations, Earth Planet. Sc. Lett., 191, 267-282, doi: 10.1016/S0012-821x(01)00424-1, 2001.

465 Jensen, J., Glasbey, C., and Corbett, P.: On the interaction of geology, measurement, and statistical analysis of small-scale permeability measurements, Terra Nova, 6, 397-403, doi: 10.1111/j.1365-3121.1994.tb00513.x, 1994.

Kling, T., Huo, D., Schwarz, J. O., Enzmann, F., Benson, S., and Blum, P.: Simulating stress-dependent fluid flow in a fractured core sample using real-time X-ray CT data, Sol. Ea., 7, 1109-1124, doi: 10.5194/se-7-1109-2016, 2016.

Kling, T., Schwarz, J.-O., Wendler, F., Enzmann, F., and Blum, P.: Fracture flow due to hydrothermally induced quartz
470   growth, Adv. Water Resour., 107, 93-107, doi: 10.1016/j.advwatres.2017.06.011, 2017.

Konzuk, J. S. and Kueper, B. H.: Evaluation of cubic law based models describing single-phase flow through a rough-walled fracture, Water Resour. Res., 40, doi: 10.1029/2003WR002356, 2004.

Matsuki, K.: Size effect in flow conductance of a small-scale hydraulic fracture in granite, Geoth. Sci. Tech., 6, 113-138, 1999.

475 Milsch, H., Spangenberg, E., Kulenkampff, J., and Meyhöfer, S.: A new apparatus for long-term petrophysical investigations on geothermal reservoir rocks at simulated in-situ conditions, Transport Porous Med., 74, 73-85, doi: 10.1007/s11242-007-9186-4, 2008.

Milsch, H., Hofmann, H., and Blocher, G.: An experimental and numerical evaluation of continuous fracture permeability measurements during effective pressure cycles, Int. J. Rock Mech. Min. Sci., 89, 109-115, doi:
480   10.1016/j.ijrmms.2016.09.002, 2016.

Mourzenko, V. V., Thovert, J.-F., and Adler, P. M.: Permeability of a single fracture; validity of the Reynolds equation, J. Phys. II, 5, 465-482, doi: 10.1051/jp2:1995133, 1995.

Nemoto, K., Watanabe, N., Hirano, N., and Tsuchiya, N.: Direct measurement of contact area and stress dependence of anisotropic flow through rock fracture with heterogeneous aperture distribution, Earth Planet Sci. Lett., 281, 81-87, doi: 10.1016/j.epsl.2009.02.005, 2009.

485

Neuzil, C. E. and Tracy, J. V.: Flow through fractures, Water Resour. Res., 17, 191-199, doi: 10.1029/WR017i001p00191, 1981.

New England Research, TinyPerm 3: available at: https://www.ner.com/site/systems/tinyperm3.html, 2015.

Ogilvie, S., Isakov, E., Taylor, C., and Glover, P.: Characterization of rough-walled fractures in crystalline rocks, Geol. Soc.

490

London, Special Publications, 214, 125-141, 2003.

Ogilvie, S. R., Isakov, E., and Glover, P. W.: Fluid flow through rough fractures in rocks. II: A new matching model for rough rock fractures, Earth Planet. Sc. Lett., 241, 454-465, doi: 10.1016/j.epsl.2005.11.041, 2006.

Possemiers, M., Huysmans, M., Peeters, L., Batelaan, O., and Dassargues, A.: Relationship between sedimentary features and permeability at different scales in the Brussels Sands, Geol. Belg., 15, 156-164, 2012.

495 Renshaw, C. E.: On the relationship between mechanical and hydraulic apertures in rough-walled fractures, J. Geophys. Res., 100, 24629-24636, doi: 10.1029/95JB02159, 1995.

Renshaw, C. E., Dadakis, J. S., and Brown, S. R.: Measuring fracture apertures: A comparison of methods, Geophys. Res. Lett., 27, 289-292, doi: 10.1029/1999GL008384, 2000.

Rogiers, B., Beerten, K., Smeekens, T., Mallants, D., Gedeon, M., Huysmans, M., Batelaan, O., and Dassargues, A.:

500

Derivation of flow and transport parameters from outcropping sediments of the Neogene aquifer, Belgium, Geol. Belg., 16, 129-147, 2013.

Rogiers, B., Beerten, K., Smeekens, T., Mallants, D., Gedeon, M., Huysmans, M., Batelaan, O., and Dassargues, A.: The usefulness of outcrop analogue air permeameter measurements for analyzing aquifer heterogeneity: quantifying outcrop hydraulic conductivity and its spatial variability, Hydrol. Process., 28, 5176-5188, doi: 10.1002/hyp.10007, 2014.

505 Saadi, F. A., Wolf, K.-H., and Kruijsdijk, C. v.: Characterization of Fontainebleau sandstone: quartz overgrowth and its impact on pore-throat framework, J. Pet. Environ. Biotechnol., 08, 1-12, doi: 10.4172/2157-7463.1000328, 2017.

Snow, D. T.: Anisotropie permeability of fractured media, Water Resour. Res., 5, 1273-1289, doi: 10.1029/WR005i006p01273, 1969.

Snow, D. T.: The frequency and apertures of fractures in rock, Int. J. Rock Mech. Min. Sci., 7, 23-40, doi: 10.1016/0148-

510

9062(70)90025-2, 1970.

Tsang, Y.: Usage of "equivalent apertures" for rock fractures as derived from hydraulic and tracer tests, Water Resour. Res., 28, 1451-1455, 1992.

Ukar, E., Laubach, S. E., and Hooker, J. N.: Outcrops as guides to subsurface natural fractures: Example from the Nikanassin Formation tight-gas sandstone, Grande Cache, Alberta foothills, Canada, Mar. Petrol. Geol. 103, 255-275,

515

2019.

Walsh, J.: Effect of pore pressure and confining pressure on fracture permeability, Int. J. Rock Mech. Min. Sci. & Geomech. Abstr., 18, 429-435, doi: 10.1016/0148-9062(81)90006-1, 1981.

Watkins, H., Bond, C. E., Healy, D., and Butler, R. W.: Appraisal of fracture sampling methods and a new workflow to characterise heterogeneous fracture networks at outcrop, J. Struct. Geol., 72, 67-82, doi: 10.1016/j.jsg.2015.02.001, 2015.

520 Witherspoon, P. A., Wang, J. S., Iwai, K., and Gale, J. E.: Validity of cubic law for fluid flow in a deformable rock fracture, Water Resour. Res., 16, 1016-1024, doi: 10.1029/WR016i006p01016, 1980.

Xiong, X., Li, B., Jiang, Y., Koyama, T., and Zhang, C.: Experimental and numerical study of the geometrical and hydraulic characteristics of a single rock fracture during shear, Int. J. Rock Mech. Min. Sci., 48, 1292-1302, doi: 10.1016/j.ijrmms.2011.09.009, 2011.

525 Zambrano, M., Pitts, A. D., Salama, A., Volatili, T., Giorgioni, M., and Tondi, E.: Analysis of fracture roughness control on permeability using SfM and fluid flow simulations: implications for carbonate reservoir characterization, Geofluids, 2019, 1-19, doi: 10.1155/2019/4132386, 2019.

Zeeb, C., Gomez-Rivas, E., Bons, P. D., and Blum, P.: Evaluation of sampling methods for fracture network characterization using outcrops, AAPG bull., 97, 1545-1566, doi: 10.1306/02131312042, 2013.

530 Zimmerman, R. W., Kumar, S., and Bodvarsson, G. S.: Lubrication theory analysis of the permeability of rough-walled fractures, Int. J. Rock Mech. Min. Sci. & Geomech. Abstr., 28, 325-331, doi: 10.1016/0148-9062(91)90597-F, 1991.

Zimmerman, R. W., Chen, D.-W., and Cook, N. G.: The effect of contact area on the permeability of fractures, J. Hydrol., 139, 79-96, doi: 10.1016/0022-1694(92)90196-3, 1992.